TRANSVERSE-TO-LONGITUDINAL EMITTANCE-EXCHANGE WITH AN ENERGY CHIRPED BEAM

J. Thangaraj*, J. Ruan, A. S. Johnson, R. Thurman-Keup, A. H. Lumpkin,
J. Santucci, Y-E. Sun, T. Maxwell, H. Edwards
Fermi National Accelerator Laboratory, IL, USA

Abstract

Emittance exchange has been proposed to increase the performance of free electron lasers by tailoring the phase space of an electron beam. The principle of emittance exchange - where the transverse phase space of the electron beam is exchanged with the longitudinal phase space - has been demonstrated recently at the A0 photoinjector. The experiment used a low charge bunch (250 pC) with no energy chirp. Theory predicts an improvement in the emittance exchange scheme when the incoming beam has an energy chirp imparted on it. The energy chirp helps to overcome the thick lens effect of the deflecting mode cavity and other second order effects that might lead to an incomplete emittance exchange at higher charges. In this work, we report experimental and simulation results from operating the emittance exchange beam line using an energy chirped beam with higher charge (500 pC) at different RF-chirp settings.

INTRODUCTION

At the Fermilab A0 photoinjector, a proof-of-principle experiment of an emittance-exchange scheme has been demonstrated recently [1]. The emittance-exchange line consists of a TM_{110} cavity sandwiched by doglegs, a variation of the original scheme proposed by Cornacchia and Emma [2], where the cavity was in the middle of a chicane. While the emittance exchange at 250 pC with no-RF chirp was close to 1:1 [1], the emittance exchange at higher charges may not be exact due to several reasons. One is the finite length of the TM_{110} cavity (thick lens effect) that introduces coupling between the incoming longitudinal phase space and the outgoing transverse phase space and vice versa. Other reasons include coherent synchrotron radiation, space-charge effects and wakefields. The thick-lens effect can be reduced by imparting an energy chirp on the beam [3]. In this work, we report on the experimental results from operating the emittance exchanger using an energy-chirped beam.

THICK LENS EFFECT

The final rms emitances after the emittance exchange beam line can be written as follows:

$$\varepsilon_{x,out}^2 = \varepsilon_z^2 + (\tfrac{17\lambda^2}{40D})^2\langle x'^2\rangle\left[\langle z^2\rangle + \alpha^2 D^2\langle\delta^2\rangle + 2\alpha D\langle z\delta\rangle\right]$$

$$\varepsilon_{z,out}^2 = \varepsilon_x^2 + (\tfrac{17\lambda^2}{40D})^2\langle x'^2\rangle\left[\langle z^2\rangle + \alpha^2 D^2\langle\delta^2\rangle + 2\alpha D\langle z\delta\rangle\right]$$

* jtobin@fnal.gov

where αD is the longitudinal dispersion, x', z, and δ are the incoming x-angle, longitudinal position, energy spread of the beam, respectively, λ is the wavelength of the cavity and D is the dispersion of a single dogleg. Thus, in the emittance exchange beamline, if we assume a thick lens cavity, the outgoing emittance is coupled with the incoming emittance [1]. In order to overcome the thick lens effect, we introduce a linear correlation between the energy and longitudinal position of the beam, $\delta = hz$, where $h = \frac{-1}{\alpha D}$. Then the last term in the equation will be minimized leading to an improvement in the emittance exchange. This is the motivation behind this work.

R-matrix

The complete R-matrix (x, x', z, δ) of the emittance exchanger, including the finite length of the cavity, can be written as follows:

$$\begin{pmatrix} 0 & \frac{Lc}{4} & \frac{-(4L+Lc)}{4\eta} & \eta-\alpha\frac{4L+Lc}{4} \\ 0 & 0 & \frac{-1}{\eta} & -\alpha \\ -\alpha & \eta-\alpha\frac{4L+Lc}{4} & \frac{\alpha Lc}{4\eta} & \frac{\alpha^2 Lc}{4\eta} \\ \frac{-1}{\eta} & \frac{-(4L+Lc)}{4\eta} & \frac{\alpha Lc}{4\eta^2} & \frac{\alpha Lc}{4\eta} \end{pmatrix}$$

where α is the bending angle of the dipoles, Lc is the length of the deflecting cavity, η is the dispersion of a dogleg, and L the length of the dogleg. When the RF-chirp is set to $\frac{-1}{\alpha\eta}$, the R-matrix is instead written as:

$$\begin{pmatrix} 0 & \frac{Lc}{4} & \frac{-1}{\alpha} & \eta-\alpha\frac{4L+Lc}{4} \\ 0 & 0 & 0 & -\alpha \\ -\alpha & \eta-\alpha\frac{4L+Lc}{4} & 0 & \frac{\alpha^2 Lc}{4\eta} \\ \frac{-1}{\eta} & \frac{-(4L+Lc)}{4\eta} & 0 & \frac{\alpha Lc}{4\eta} \end{pmatrix}$$

As can be seen in the above matrix, both the R_{33} and R_{43} elements are reduced to zero from the original matrix due to the chirp. This leads to a reduction in the bunchlength and the energy spread after the emittance exchanger. In the transverse plane both the R_{13} and R_{23} terms are also reduced due to the chirp indicating possible reduction in beam size and beam divergence as well.

SECOND ORDER EFFECTS

A positive side-effect of using a chirped beam is the decrease in the x' after the cavity. Recall that after the cavity, $\Delta x' = \kappa\Delta z$, where κ is the strength of the deflecting cavity set to $\frac{-1}{\eta}$ for EEX. So if we reduce the bunch length at the cavity by adding energy chirp, the beam divergence

Copyright © 2012 by IEEE – cc Creative Commons Attribution 3.0 (CC BY 3.0) — cc Creative Commons Attribution 3.0 (CC BY 3.0)

ISBN 978-3-95450-115-1

after the cavity is also reduced and thus reducing the emittance growth from second order dispersive aberration. A negative side effect of using a chirped beam is the increase in coherent radiation effects that can spoil the transverse emittance of the beam in the bend plane. Coherent radiation effects increase quadratically with charge and limits our experiment to 400 pC, where the coherent radiation effects are not a significant threat as compared to higher charges [4].

EXPERIMENTAL SETUP

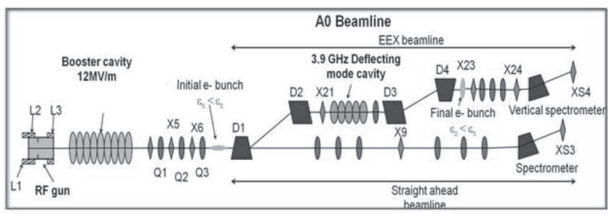

Figure 1: Schematic of the A0 photoinjector facility.

The A0 Photoinjector (A0PI) facility shown in Fig. 1 consists of a 1.5-cell normal conducting L-band RF photoinjector driven by the UV component of a Nd: glass drive laser. The L-band RF gun is followed by a superconducting booster cavity, which accelerates the e-beam up to 16 MeV. After acceleration, the beam can either be sent to a straight ahead beamline or the emittance exchange beamline. The straight ahead beamline consists of quadrupole triplet followed by a horizontal spectrometer (XS3). The emittance exchange beamline consists of the doglegs (D1, D2, D3, D4) followed by a quadrupole triplet and a vertical spectrometer (XS4). Between the doglegs is the horizontal deflecting cavity, which is a liquid-Nitrogen-cooled five-cell copper cavity operating on the TM_{110} mode at 3.9 GHz.

Diagnostics

Precise measurements of beam parameters are important to verify the emittance exchange principle. A detailed list of the diagnostics and upgrades are given in [5]. The beam size is measured using either optical transition radiation (OTR) screens or YAG:Ce scintillator screens installed throughout the beamline. The transverse emittances of the e-beam are measured using the multi-slit technique at X3 and X23 using a MATLAB-based Graphical User Interface (GUI)[6]. The incoming and the outgoing bunch length (σ_z) is measured at X9 and X24, respectively, using the OTR light that is transported to a Hamamatsu C5680 streak camera. The bunch length at X24 can also be measured using a Martin-Puplett interferometer using coherent transition radiation (CTR). The energy spread, σ_δ, is measured using a spectrometer magnet followed by a screen. The longitudinal emittance is calculated as the product of the minimum energy spread and the bunch length, i.e. $\sigma_\delta \sigma_z$. This is the upper-limit for the longitudinal emittance.

REDUCTION OF THE E-BEAM BUNCH LENGTH

If adding chirp mitigates the thick-lens effect, then the bunch length of the electron beam must also be reduced due to the minimization of the R_{33} term. In order to investigate this, we imparted an energy-chirp on the beam by operating the 9-cell off-crest and measured the bunch length of the electron beam at X24 with a streak camera. For Q3 set between 0.35 to 0.55 A, the bunch length reached the resolution limit of the streak camera (∼300 fs), as shown in Fig. 2. We then did CTR power measurements with the pyrodetector for a beam with and without chirp, as shown in Fig. 3. The results showed a factor of 2 increase in the power detected for a beam with RF chirp which indicates a reduction in bunch length. Finally, the bunch length of the electron beam, with and without chirp, was measured using a Martin-Puplett interferometer, as shown in Fig. 4 demonstrating a factor of 2 compression.

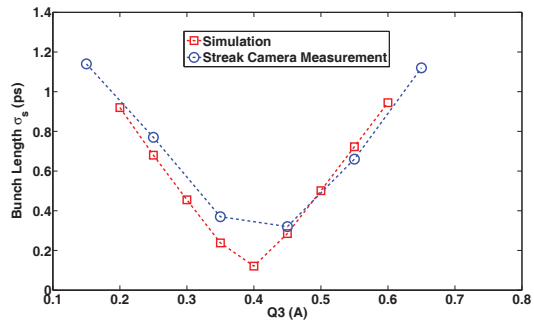

Figure 2: Comparison of bunch lengths of the electron beam measured at X24 using a streak camera as a function of quadrupole (Q3) current versus those of simulation. The chirp was set to -40 degrees off-crest.

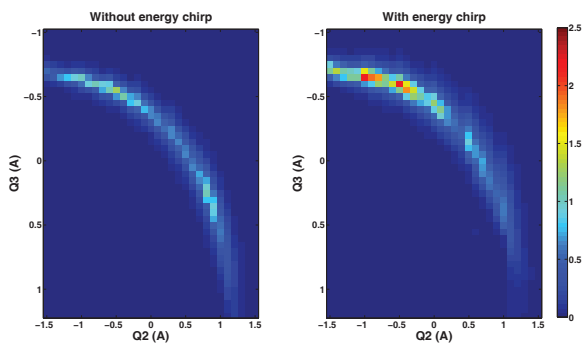

Figure 3: Pyrodetector measurements of coherent transition radiation at X24 as a function of upstream quadrupoles Q2 and Q3. No energy chirp on the beam (left) and with an energy chirp on the beam (right) at 40 degrees off crest.

EXPERIMENTAL RESULTS

In this experiment, the beam energy was set to 13.2 MeV. This was done to maintain the same beam energy for different RF-phase settings without driving the gradient too high

Copyright © 2012 by IEEE – cc Creative Commons Attribution 3.0 (CC BY 3.0) — cc Creative Commons Attribution 3.0 (CC BY 3.0)

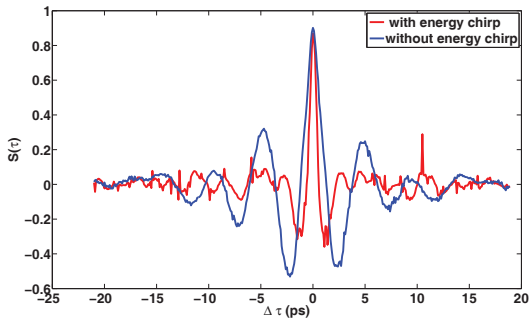

Figure 4: Auto-correlation measurement with Martin-Puplett interferometer with and without energy chirp.

on the 9-cell cavity. The charge per bunch was 400-450 pC. The incoming rms normalized transverse emittance was 4 μm. The incoming bunch length was measured at X9 using a streak camera and the minimum energy spread was measured using a RF-phase scan and the spectrometer magnet in the straigh ahead beamline. The rms normalized longitudinal emittance was 20 μm. The beam was then sent through the emittance exchange line and the transverse and the longitudinal emittances were measured after the exchange. The results of the measurement for different chirp setting are shown in Fig. 5. The emittance exchange ratio improves as the RF chirp on the beam increases. Ideally, the ratio should be one, but higher order effects in the dogleg, non-linearities in the field in the deflecting cavity, and space-charge effects could limit the achievable ratio in the laboratory.

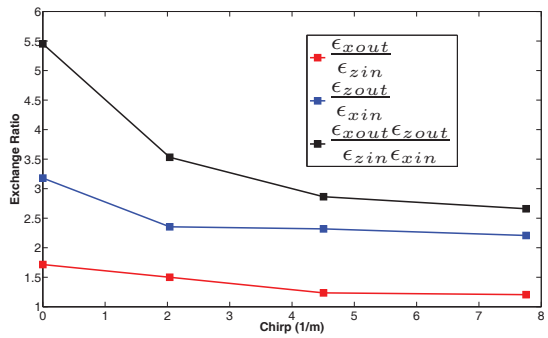

Figure 5: Measured value of the emittance exchange ratio and their products. As the RF-chirp increases, the ratio tends towards one. There is still some emittance dilution possibly due to second order effects and space charge.

SIMULATION

General Particle Tracker (GPT) simulations were done to model the emittance exchange process with an energy chirped beam. The measured Twiss parameters and the beam parameters were used as the initial conditions at X3. The booster cavity chirp was adjusted through the program, which used a Gaussian distribution (in transverse) and a flat-top (in longitudinal), to model the beam in 6-D phase-space with 10k particles. In order to simulate the dogleg dipole, the measured field map was used. The deflecting cavity was modeled using a 3D-field map obtained from an electro-magnetic field solver. The results of the simulation for different RF-chirp settings are shown in Fig. 6. There is a difference in the predicted RF-phase (of about 5-degrees) between the simulation and the measurement that minimizes the exchange ratio. Further analysis is being done to study this difference.

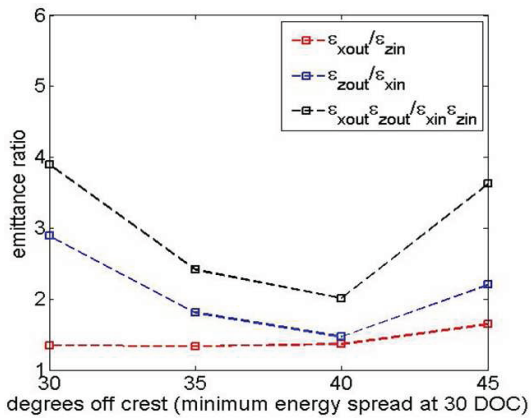

Figure 6: Simulated value of the emittance exchange ratio and their products using GPT.

SUMMARY AND CONCLUSION

We have reported experimental results from operating the emittance exchange beam line using an energy-chirped beam at different energy-chirp settings. The emittance exchange ratio decreases as a function of increasing chirp as predicted by the theory upto a certain chirp value and then increases again. Results from these studies will be incorporated for designing a chicane-style emittance exchanger for the Advanced Superconducting Test Accelerator (ASTA) at 40 MeV.

ACKNOWLEDGMENTS

We thank the A0 technical support team. We also thank M. Church, V. Shiltsev, M. Wendt and P. Piot for their interest and encouragement. This work was supported by the Fermi Research Alliance, LLC under the U.S. Department of Energy.

REFERENCES

[1] J. Ruan, et al., PRL, vol. 106, no. 24, p. 244801, 2011.

[2] M. Cornacchia and P. Emma, *PRSTAB*, vol. 5, p. 084001, 2002.

[3] P. Emma, et. al. *PRSTAB*, vol. 9, p. 100702, 2006.

[4] Jayakar C. T. Thangaraj, et. al, FEL 2011, Shanghai, 2011.

[5] A. Lumpkin, et al. PRSTAB, vol. 14, no. 6, p. 060704, 2011.

[6] R. Thurman-Keup et. al, PAC 2011, New York, 2011.

Copyright © 2012 by IEEE – cc Creative Commons Attribution 3.0 (CC BY 3.0) — cc Creative Commons Attribution 3.0 (CC BY 3.0)

ISBN 978-3-95450-115-1